Journal of Advanced Research in Ocean Engineering 1(4) (2015) 239-251
http://dx.doi.org/10.5574/JAROE.2015.1.4.239

Spectral Fatigue Analysis for Topside Structure of Offshore Floating Vessel †

Dae-Ho Kim [1*], Jae-Woo Ahn [1], Sung-Gun Park [1], Seock-Hee Jun [1], and Yeong-Tae Oh [1]

[1]*Ship & Ocean R&D Institute, Daewoo Shipbuilding & Marine Engineering Co., Ltd., Seoul, Korea*

(Manuscript Received September 9 2015; Revised October 30, 2015; Accepted November 30, 2015)

Abstract

In this study, a spectral fatigue analysis was performed for the topside structure of an offshore floating vessel. The topside structure was idealized using beam elements in the SACS program. The fatigue analysis was carried out considering the wave and wind loads separately. For the wave-induced fatigue damage calculation, motion RAOs calculated from a direct wave load analysis and regular waves with different periods and unit wave heights were utilized. Then, the member end force transfer functions were generated covering all the loading conditions. Stress response transfer functions at each joint were produced using the specified SCFs and member end force transfer functions. fatigue damages were calculated using the obtained stress ranges, S-N curve, wave spectrum, heading probability of each loading condition, and their corresponding occurrences in the wave scatter diagrams. For the wind induced fatigue damage calculation, a dynamic wind spectral fatigue analysis was performed. First, a dynamic natural frequency analysis was performed to generate the structural dynamic characteristics, including the eigenvalues (natural frequencies), eigenvectors (mode shapes), and mass matrix. To adequately represent the dynamic characteristic of the structure, the number of modes was appropriately determined in the lateral direction. Second, a wind spectral fatigue analysis was performed using the mode shapes and mass data obtained from the previous results. In this analysis, the Weibull distribution of the wind speed occurrence, occurrence probability in each direction, damping coefficient, S-N curves, and SCF of each joint were defined and used. In particular, the wind fatigue damages were calculated under the assumption that the stress ranges followed a Rayleigh distribution. The total fatigue damages were calculated from the combination with wind and wave fatigue damages according to the DNV rule.

Keywords: topside structure; spectral fatigue analysis; motion RAO; dynamic wind spectral fatigue analysis

1. Introduction

Offshore oil fields have been developed since the mid-1900s. At that time, all of the oil platforms were installed on the seabed. However, oil exploration moved to deeper waters and more distant locations from onshore in the 1970s. Thus, floating production and storage systems were used. In these offshore floating facilities, the fatigue strength of the topside structure and hull structures is the one of the most important design requirements because of the long design life and exposure to environmental loads during the operat-

† This paper was presented at the 25th International Ocean and Polar Engineering Conference, Kona, Big Island, Hawaii, USA, June, 2015.

*Corresponding author. Tel.: +82-2-2129-3553
E-mail address: dhkim76@DSME.co.kr

ing period.

This paper introduces the overall procedures for a spectral fatigue analysis of the topside structure of an offshore floating vessel with wave and wind loads. The details used in the analysis and the analysis results with comparisons of the wave and wind induced damage are shown. The purpose of the spectral fatigue analysis was to confirm the fatigue strength of the considered structure under the given environmental loads and the contribution of each wind and wave load to the total fatigue damage.

2. Procedure

The spectral fatigue analyses were performed separately for the wave and wind-induced loads acting on a topside structure. The fatigue damage was calculated in the frequency domain utilizing probabilistic spectral techniques, the global finite beam element model in SACS, and Miner's rule to calculate the accumulated damage from different environmental data. Detailed descriptions of the wind and wave-induced fatigue damage calculations are shown in the following sections.

3. Fatigue Damage Calculation for Wave Loads

The fatigue analysis considering wave-induced loads was carried out in the SACS program using motion RAOs calculated from a direct wave load analysis. The inertial loads were applied to the finite element (FE) model using the motion RAO data for the displacement amplitudes, covering all loading conditions and specific wave directions in order to establish transfer functions. A series of regular waves with different periods and unit wave heights was selected to generate the transfer functions, and 16 steps were used for each wave period to determine the maximum and minimum values. The selected wave periods covered the range of 4.0–40.0 s, according to the motion RAO data. The center of motion corresponded to the RAO data for each loading condition. The member end forces were calculated under inertial loads.

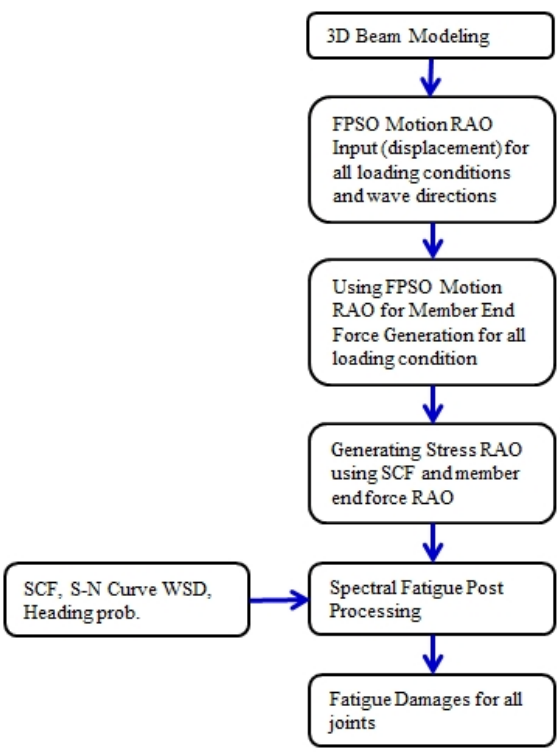

Fig.1. Overall procedure of fatigue damage calculation for wave loads

Appropriate stress concentration factors and S-N curves needed to be defined in accordance with the joint types of the structures. In SACS, stress concentration factors (SCF) are calculated automatically for tubular joints per the specified DNV recommended practice (DNV, RP-C203, 2012). A detailed description is given in the next section. In this study, for a non-tubular joint, an SCF of 5 and an F3 curve were applied as a conservative approach based on industrial experience. The stress response transfer functions at each joint were produced using the specified stress concentration factors and member end force transfer functions. The wave scatter diagrams and heading probability were also used according to site specific data. Fatigue damages were calculated using the obtained stress ranges, S-N curve, wave spectrum (JONSWAP), heading probability, and their corresponding occurrences in the wave scatter diagrams for all the loading conditions. The overall procedure for the analysis of the fatigue by wave-induced loads is shown in Fig. 1.
The major wave fatigue parameters are described in the following sections.

3.1 Wave Periods and Heading Angles

Wave periods in the range of 4.0–40.0 s were considered.
The heading probability for each loading condition was considered in accordance with the heading analysis results. For a fatigue life estimation, in this study, a heading angle with a 15° increase was considered from 0–360°.

3.2 Wave Spectrum and Scatter Diagram

Based on the Metocean information for the target vessel's operating location, a wave scatter diagram and JONSWAP spectrum were used, as shown in Eq. 1.

$$S(f) = \alpha g^2 (2\pi)^{-4} f^{-5} \exp\left(-5/4\left(\frac{f}{f_p}\right)^{-4}\right) \gamma^{\exp\left(-\frac{(f-f_p)^2}{2\sigma^2 f_p^2}\right)} \quad (1)$$

where = 0.07 for $f \leq f_p$
= 0.09 for $f > f_p$
f_p = Peak frequency
= peakedness parameter

3.3 Hydrodynamic Analysis (Motion RAO)

Motion RAOs in terms of the displacement amplitudes were calculated from the hydrodynamic analysis results. A hydrodynamic analysis to establish the dynamic features of the vessel was carried out using a 3D panel method program. All of the responses were represented in the frequency domain. The dynamic wave load and motion-induced loads were calculated for each wave in unit amplitude and applied to the structural FE model.

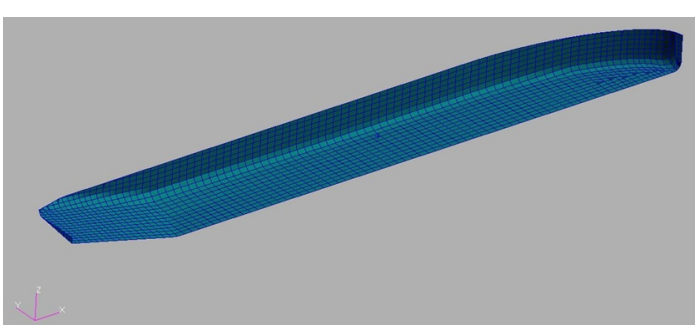

Fig. 2 3D Sink-source half breadth model

The DNV software WADAM (WAve loading by Diffraction And Morison theory) was used in the hydrodynamic analysis. It is a general hydrodynamic analysis program for the calculation of wave loads and the wave-induced responses of fixed and floating offshore structures in the frequency domain. WADAM is based on a 3D sink-source (diffraction-radiation) method coupled to a Morison equation. It has a useful capability of allowing viscous forces to be incorporated in the modeling, which is important for the roll motion of a vessel. The 3D sink-source model was generated using shell elements, as shown in Fig. 2.

Generally, a motion analysis uses a mass model constructed of mass elements with appropriate distributions in the X, Y, and Z directions to obtain the same COG (center of gravity) as the actual condition. If the radius of gyration, especially the roll radius of gyration, is known, the mass elements in the mass model can be arranged to have the same roll radius of gyration. However, it is not easy to predict that value. In this study, instead of adopting a mass model made of point mass elements, the FE models to be analyzed were used as mass models to correctly predict the radius of gyration and minimize any possible unbalance force as follows,

1. For the hull structure, the steel density was adjusted along the X and Z directions to obtain the same COG with each loading condition.
2. For each topside structure, tank, and other compartments, mass elements were distributed to have the same mass distribution with each loading condition.
3. For each loading condition, different FE models with the same stiffness but different mass distributions were created for the wave load analysis.

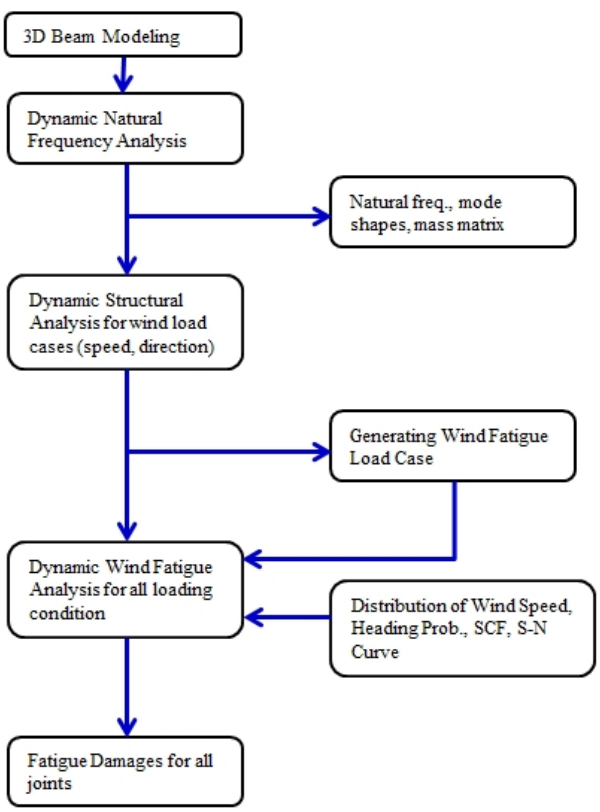

Figure 3 Overall procedure of fatigue damage calculation for wind loads

4. Fatigue Damage Calculation for Wind Loads

The dynamic wind spectral fatigue analysis was performed using the SACS program.

The first step of the dynamic wind spectral fatigue analysis was to perform a dynamic natural frequency analysis using the SACS-DYNPAC program. The DYNPAC program module generated structural dynamic characteristics, including eigenvalues (natural frequencies), eigenvectors (mode shapes), and a mass matrix, in order to carry out a dynamic structural analysis. To adequately represent the dynamic characteristics of the structure, the number of modes was determined to ensure that the cumulative mass participation factor was at least greater than 95% in the lateral direction. The vertical direction mass participation was not important because most damage occurs in the lateral modes.

The next step was to run the dynamic structural analysis and wind spectral fatigue analysis using the mode shapes and mass data obtained from the previous DYNPAC results. This run created a fatigue input file that included the fatigue load data in conjunction with the mode participation factors. The fatigue module was automatically executed. In this input file, the Weibull distribution of the wind speed, probability of occurrence in each direction, damping coefficient, S-N curves, and SCF were defined. Fatigue damages were calculated using the fatigue parameters for all the loading conditions. The overall procedure for the analysis of the fatigue by wind-induced loads is shown in Fig. 3.

The major wind fatigue parameters are described in the following sections.

4.1 Wind Loading

The wind loading was specified in twelve directions at 30° intervals, with a sufficient number of wind speed bands between 1 m/s and 27 m/s, to describe the shape of the Weibull distribution function.

The heading probability for each loading condition was considered in accordance with the heading analysis results.

These wind loads were used, together with the mode shapes and modal mass from the natural frequency analysis, to calculate the response spectrum using the Harris Wind Spectrum.

4.2 Harris Wind Spectrum

The Harris wind spectrum shall be used in the SASC program to describe the dynamic wind behavior. The Harris spectrum is given by Eq. 2.

$$S_V(f) = V_{10}^2 \frac{4k\eta_1(f)}{(2+\eta_1^2(f))^{\frac{5}{6}}} \tag{2}$$

where $\eta_1(f) = f(\frac{L_H}{v_{10}})$

V_{10} =10-min mean wind speed, 10 m above sea level

k = surface roughness parameter

L_H =Integral scale length parameter, f = frequency

The surface roughness for open seas is dependent on the wave height and consequently the mean wind speed. A value of 0.003 m was used based on the DNV rule (DNV, RP-C205, 2007). The scale length parameter was taken to be 1800 m, which was the mean value for the Harris spectrum.

4.3 Wind Speed Occurrence

The Weibull distribution is often used as the parent distribution for wind speed. In SACS, the long-term distribution of the wind speed is given as a Weibull distribution. The Weibull distribution of the wind speeds is defined in Eq. 3.

$$\mathrm{P}(V) = 1 - \exp[-\left(\frac{V}{a}\right)^{k}] \tag{3}$$

where a = Weibull scale parameter (6.5),
k = Weibull shape parameter (2.5),
V = Wind speed

The wind speed distribution was considered to be the basis for fitting a Weibull distribution curve. In this study, Weibull scale and shape parameters of 6.5 and 2.5 were applied, respectively, according to the wind scatter diagram for the target location.

4.4 Generalized Force Spectrum

The generalized force spectrum used for the spectral wind fatigue analysis consisted of the Harris wind spectrum, gust effect spatial correlation, and mean wind velocity variation. For any mode (i), the generalized force spectrum S_i(f) is taken as Eq. 4.

$$S_i(f) = \frac{4}{f} F_i^2 J_{ai}(f) J_{rt}^2(f) S_V(f) \tag{4}$$

where F_i = generalized force for each mode,
S_V (f) = the Harris spectrum
J_{ai} = mean wind velocity variation function
J_{rt} = gust effects spatial correlation function

The response for each mode is calculated from the RMS (Root Mean Square) of the generalized force spectrum and mechanical transfer function.

4.5 Mechanical Transfer Function

The mechanical transfer function is given in Eq. 5.

$$H_i(n)^2 = \frac{1}{K_i^2}[\left(1 - \left(\frac{n}{n_i}\right)^2\right)^2 + \left(2 \cdot c_i \frac{n}{n_i}\right)^2]^{-1} \tag{5}$$

where K_i = generalized modal stiffness,
n_i = natural frequency, c_i = applied damping ratio

4.6 Damping Coefficient

The damping is given as a fraction of the critical value. Usually a value of 0.01 is applied, where 0.005 is the contribution from the structural damping, and 0.005 is the aerodynamic damping.

4.7 Assumption for Wind Fatigue Damage Calculation

For the wind spectral fatigue analysis in SACS, it was assumed that the response was a Gaussian process, and this process was narrow-banded. This means that the stress range could also be assumed to follow a

Table 1 Weight and COG information of target topside structure

Description	Weight (ton)	COG(m)		
		X	Y	Z
Structure Weight	21.9	289.6	18.9	80.6
Variable Functional Load	10.1	289.7	18.9	81.8
Total	32.0	289.6	18.9	81.0

Rayleigh distribution, taking into account the linear relationship between the wind spectrum and response spectrum.

5. FE Model and Boundary Condition

The target topside FE model used a three-dimensional beam in SACS, as shown in Fig. 4. Fixed boundary conditions were applied to the bottom of the FE model.

6. Weight Information

The weight information of the topside structure and the center of gravity are summarized in Table 1. Each weight was distributed in the FE model following Table 1.

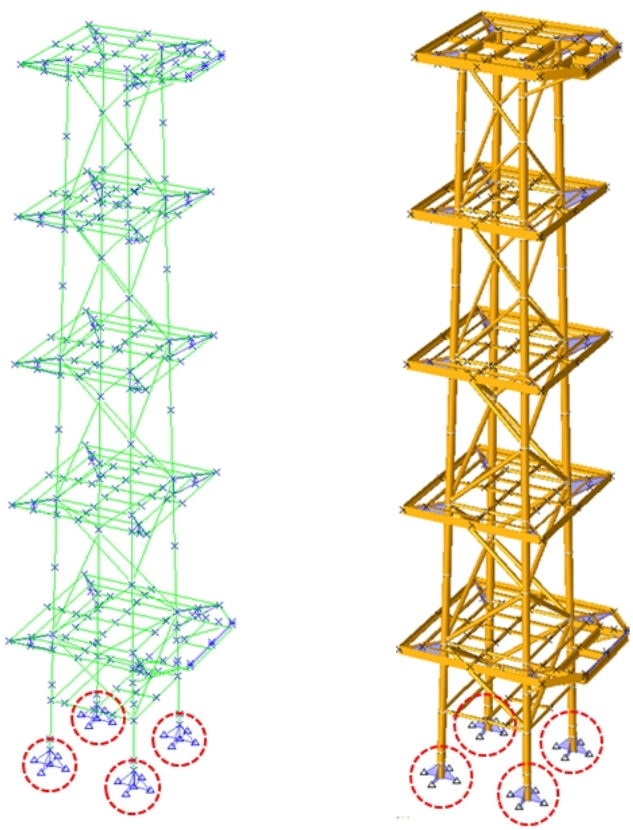

Fig. 4 Wireframe (left) and solid element (right) views of global FE model

Table 2 Fatigue loading condition

Loading condition	Mean Draft (m)	GM (m)
Min. Operation Draft	13.54	3.73
Intermediate Draft	16.66	2.96
Max. Operation Draft	21.15	2.62

Table 3 S-N Curves in Air

S-N Curves	$N \leq 10^7$ cycles		$N \leq 10^7$ cycles log $\bar{a}_2$	Fatigue limit	Thickness
	m_1	log $\bar{a}_1$	$m_2 = 5.0$	at 10^7 cycles	exponent k
D	3.0	12.164	15.606	52.63	0.2
T	3.0	12.164	15.606	52.63	0.25
F3	3.0	11.546	14.576	32.75	0.25

7. Loading Condition

A few representative loading conditions were selected for fatigue analyses from the Trim & Stability Booklet. Generally, in contrast to a strength calculation, the loading conditions for a fatigue calculation are selected from among frequently occurring conditions or the most dominant conditions from a duration point of view. Among the possible frequent conditions, representative conditions were selected based on the draft and GM values to maximize the draft change and transverse acceleration as much as possible. The selected loading conditions are summarized in Table 2.

Regarding the wind fatigue damage calculation, the vertical location of the topside structure above the sea surface was changed according to the draft of each loading condition. Therefore, the draft of the vessel under each loading condition was major input data because of the change in the wind velocity under the boundary layer, which was generally 275 m above the mean sea level.

8. S-N CURVE

The S-N curves were selected in accordance with the DNV recommended practice (DNV, RP-C203, 2012). For all tubular and non-tubular joints, the F3 curve was used in the fatigue damage estimation. This was a very conservative approach because in the SACS program, the fatigue damage is calculated based on a hot spot stress approach in combination with the nominal stress and SCF. In the F3 curve, the structural stress concentration embedded in the detail is 1.61, i.e., the D and T curve are 1.0, as described in the DNV recommended practice (DNV, RP-C203, 2012).

Two sloped S-N curves in the air were used for the fatigue analysis, as listed in Table 3.

The fatigue strength of welded joints is somewhat dependent on the plate thickness. This effect is due to the local geometry of the weld toe in relation to the thickness of the adjoining plates. The thickness effect was accounted for by modifying the stress using Eq. 6 for a thickness greater than the reference thickness.

$$\log N = \log \bar{a} - m \cdot \log(\Delta\sigma(\frac{t}{t_{ref}})^k) \quad (6)$$

where t_{ref} = reference thickness equal to 25 mm for welded connections. For tubular joints it is 32 mm.

k = thickness exponent on fatigue strength in Table 3.

Table 4 SCFs for representative joints by Efthymiou method

JOINT	MEMBER	JNT TYP	MEM TYP	STRESS CONCENTRATION FACTORS AX-CR	AX-SD	IN-PL	OU-PL
PFA4	PFA4-PFB1	K	BRC	1.88	1.88	2.03	2.35
PFA4	PFA4-HAB4	K	CHD	1.53	1.53	0.85	1.84
PFA4	PFA4-PFB3	K	BRC	1.96	1.96	2.0	2.45
PFA4	PFA4-HAB4	K	CHD	1.61	1.61	0.87	1.91
PFA4	PFA4-A001	K	BRC	2.91	2.91	1.87	2.72
PFA4	PFA4-HAB4	K	CHD	2.32	2.32	1.07	2.12
PFA4	PFA4-A007	K	BRC	2.93	2.93	1.87	2.74
PFA4	PFA4-HAB4	K	CHD	2.34	2.34	1.07	2.13

9. Stress Concentration Factors (Scf)

Appropriate stress concentration factors needed to be defined in accordance with the joint types of the structures. The SACS program can calculate stress concentration factors for tubular connections using numerous methods, including the most generally accepted methods used in the offshore industry. For tubular joints, the SCFs suggested by Efthymiou options are available. Therefore, the SCFs were automatically calculated in accordance with the DNV recommended practice (DNV, RP-C203, 2012).

When using the SCFs suggested by Efthymiou, the calculated SCFs for representative tubular joints, which had the maximum fatigue damage, and four types of K joints are shown in Table 4 and Fig. 5.

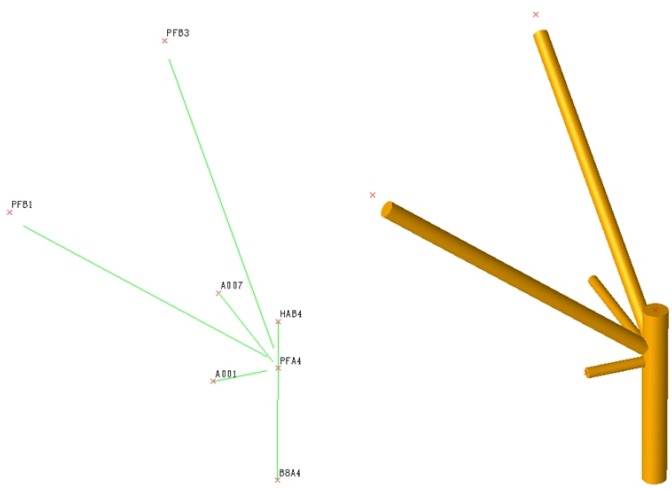

Figure 5 Wireframe (left) and solid element (right) views of K joint

10. Results

10.1 Dynamic Natural Frequency Analysis Results

The dynamic natural frequency analysis was performed for 50 modes to discover the number of modes needed to adequately represent the dynamic characteristic of the structure. Thus, the first 30 modes were selected to give cumulative mass participations of 97.98% in X, 98.03% in Y, and 90.03% in Z. The eigenvalue parameters and mass participation factors for the first ten modes are listed in Tables 5 and 6, respectively. The first mode shape is presented in Fig. 6.

Table 5 Frequency and generalized mass

Mode	FREQ. (CPS)	GEN. Mass	EIGEN VALUE	PERIOD (SECS)
1	3.271	1.04.E+01	2.37.E-03	0.306
2	3.510	1.08.E+01	2.06.E-03	0.285
3	6.276	3.51.E+01	6.43.E-04	0.159
4	8.487	2.08.E+01	3.52.E-04	0.118
5	8.816	1.91.E+01	3.26.E-04	0.113
6	16.159	1.55.E+01	9.70.E-05	0.062
7	17.213	1.96.E+01	8.55.E-05	0.058
8	18.572	1.92.E+01	7.34.E-05	0.054
9	19.910	1.17.E+01	6.39.E-05	0.050
10	20.800	6.17.E+00	5.85.E-05	0.048

Table 6 Mass participation factor

Mode	Mass participation factors			Cumulative factors		
	X	Y	Z	X	Y	Z
1	7.1.E-01	1.7.E-02	1.4.E-05	7.1.E-01	1.7.E-02	1.4.E-05
2	1.4.E-02	7.4.E-01	2.0.E-07	7.2.E-01	7.6.E-01	1.4.E-05
3	5.0.E-07	4.2.E-04	1.2.E-06	7.2.E-01	7.6.E-01	1.5.E-05
4	2.4.E-01	2.1.E-02	5.9.E-05	9.6.E-01	7.8.E-01	7.4.E-05
5	1.9.E-02	2.0.E-01	7.6.E-06	9.8.E-01	9.9.E-01	8.1.E-05
6	0.0.E+00	8.9.E-05	3.4.E-05	9.8.E-01	9.9.E-01	1.2.E-04
7	1.0.E-04	1.7.E-04	6.7.E-06	9.8.E-01	9.9.E-01	1.2.E-04
8	9.9.E-03	1.2.E-03	2.9.E-04	9.9.E-01	9.9.E-01	4.2.E-04
9	2.0.E-03	7.1.E-03	3.3.E-06	9.9.E-01	9.9.E-01	4.2.E-04
10	3.5.E-06	8.8.E-04	6.3.E-04	9.9.E-01	1.0.E+00	1.1.E-03

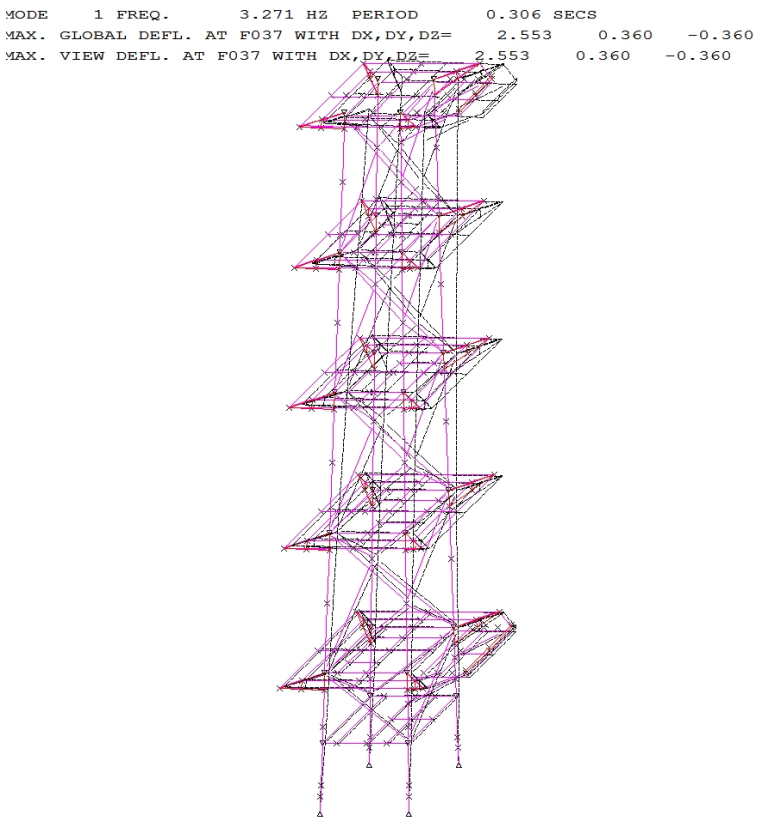

Figure 6 First mode shape of topside structure

10.2 Total Fatigue Damages

When two fatigue damages with different dynamic processes are separately calculated, it is non-conservative to simply add the two fatigue values together. From the DNV recommended practice (DNV, RP-C203, 2012), a simple method for the derivation of the resulting fatigue damages from two processes is presented as follows.

The fatigue damages from the wave and wind loads were added using Eq. 7.

$$D_{total} = D_1\left(1-\frac{v_2}{v_1}\right)+v_2\left\{\left(\frac{D_1}{v_1}\right)^{\frac{1}{m}}+\left(\frac{D_2}{v_2}\right)^{\frac{1}{m}}\right\}^m \tag{7}$$

where D_1 = calculated fatigue damage for high-frequency response
D_2 = calculated fatigue damage for low-frequency response
v_1 = mean zero up crossing frequency for high-frequency response
v_2 = mean zero up crossing frequency for low-frequency response
m = negative inverse slope of the SN curve

The top 10 joints with the maximum fatigue damage are listed in Tables 7 and 8 for tubular and non-tubular joints, respectively. The combined fatigue damage for the two-slope S-N curves was calculated using slope m = 3.0 and m = 5.0. In all the joints, the fatigue damages using m = 5.0 were bigger than those using m = 3.0.

Table 7 Minimum fatigue lives for tubular joints

JOINT	Wave Fat. Damage	Wind Fat. Damage	Comb. Fat. Damage	Fatigue Life
HAB2	6.92E-03	5.47E-05	1.72E-02	2.32E+03
HAB4	1.04E-02	5.56E-05	2.44E-02	1.64E+03
PFA2	7.79E-03	2.25E-04	2.48E-02	1.61E+03
PFA3	7.46E-03	9.54E-05	2.02E-02	1.98E+03
PFA4	8.05E-03	2.33E-04	2.56E-02	1.56E+03

Table 8 Minimum fatigue lives for non-tubular joints

JOINT	Wave Fat. Damage	Wind Fat. Damage	Comb. Fat. Damage	Fatigue Life
B001	9.72.E-04	1.57.E-06	1.91.E-03	2.09.E+04
B003	1.58.E-03	1.89.E-06	3.01.E-03	1.33.E+04
D004	6.47.E-04	4.00.E-06	1.55.E-03	2.59.E+04
E004	4.64.E-04	1.59.E-05	1.53.E-03	2.61.E+04
E006	8.06.E-04	3.79.E-06	1.84.E-03	2.17.E+04

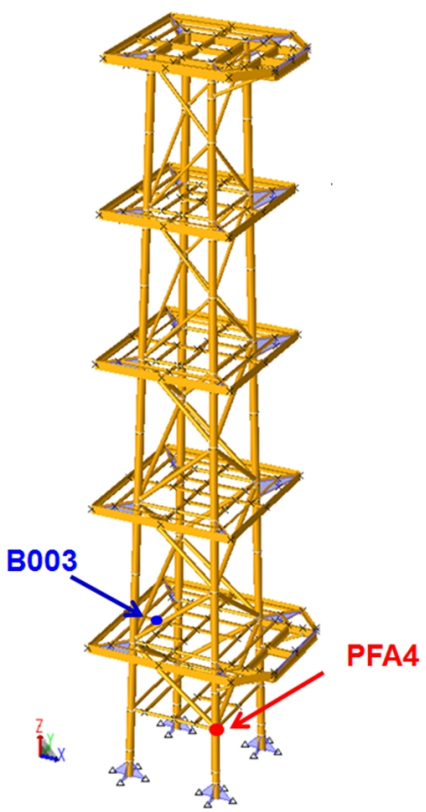

Figure 7 Minimum fatigue life locations for tubular (PFA4) and non-tubular joint (B003)

11. Conclusion

In this study, spectral fatigue analyses were performed for the topside structure of an offshore floating vessel. The fatigue analysis was carried out considering wave and wind loads separately.

The topside structure located on the top of a vessel has no direct wave loads, but inertia loads should be considered because of the vessel motion. As a result of using the motion RAO, the inertia load was easily applied to the topside FE model without the whole vessel FE model in SACS.

It could be clearly determined that the combined fatigue damage considering each frequency was more conservative than that found through simple addition. Therefore, the wind fatigue damage cannot be ignored because of the damage combination even though the wave-induced fatigue damage is much bigger than the wind fatigue damage. In addition, when m = 5, the combined fatigue damage was more conservative.

References

American Petroleum Institute, RP 2A-WSD, "Recommended Practice for Planning, Designing and Constructing Fixed Offshore Platforms- Working Stress Design", Twenty-First Edition, December 2000.

Bentley Systems Inc., SACS Manual (2012).

Det Norske Veritas, DNV-RP-C203, "Fatigue Design of Offshore Steel Structures", October 2012.

Det Norske Veritas, DNV-RP-C205, "Environmental Conditions and Environmental Loads", April 2007.

Holmes, John D (2007). *Wind Loading of Structures,* Taylor & Francis, 340.